



1     **Estimating changes of temperatures and precipitation extremes in India using the**  
2                     **Generalized Extreme Value (GEV) distribution**  
3

4     **Kishore Pangaluru<sup>1\*</sup>, Isabella Velicogna<sup>1,2</sup>, Tyler C. Sutterley<sup>1</sup>, Yara Mohajerani<sup>1</sup>,**  
5                     **Enrico Ciraci<sup>1</sup>, Jyothi Sompalli<sup>3</sup>, and Saranga Vijaya Bhaskara Rao<sup>3</sup>**  
6

7     1. Department of Earth System Science, University of California, Irvine, California,  
8         92697, USA

9     2. Jet Propulsion Laboratory, California Institute of Technology, Pasadena, California,  
10        USA

11    3. Department of Physics, Sri Venkateswara University, Tirupati, India  
12  
13  
14  
15  
16  
17  
18  
19  
20  
21  
22

23    **\*Corresponding Author:**

24    **Email: [kishore@uci.edu](mailto:kishore@uci.edu); Ph:1-949-824-3516**  
25  
26



## 27 Abstract

28 Changes in extreme temperature and precipitation may give some of the largest  
29 significant societal and ecological impacts. For changes in the magnitude of extreme  
30 temperature and precipitation over India, we used a statistical model of generalized  
31 extreme value (GEV) distribution. The GEV statistical distribution is a time-dependent  
32 distribution with different time scales of variability bounded by a precipitation, maximum  
33 ( $T_{\max}$ ), and minimum ( $T_{\min}$ ) temperature extremes and also assessed their possibility  
34 changes are evaluated and quantified over India is presented. The GEV-based method is  
35 applied on both precipitation and temperature extremes over India during the 20<sup>th</sup> and 21<sup>st</sup>  
36 centuries using multiple coupled climate models taking an interest in the Coupled Model  
37 Intercomparison Project Phase 5 (CMIP5) and observational datasets. The regional means  
38 of historical warm extreme temperatures are 34.89, 36.42, and 38.14 °C for three different  
39 (10, 20, and 50-year) periods, respectively; whereas the cold extreme mean temperatures  
40 are 7.75, 4.19, and -1.57 °C. It indicates that 20th century cold extreme temperatures have  
41 relatively larger variations than the warm extremes. As for the future, the CMIP5 models  
42 of warm extreme regional mean values increase from 0.33 to 0.75 °C in all return periods  
43 (10-, 20-, and 50-year periods), while in the case of cold extreme means values vary  
44 between 0.58 and 2.29 °C. In the future, cold extreme values have a larger increasing rate  
45 over the northwest, northeast, some parts of north central, and Inter Peninsula regions.  
46 The CRU precipitation extremes are larger than the historical extreme precipitation in all  
47 three (10, 20, and 50-year) return-periods.

48

49 Keywords: Precipitation, surface temperature, GEV, Historical, and CMIP5.



## 50 1. Introduction

51 Extreme weather events, amplified by climate change, can lead to major  
52 environmental issues affecting human society. Precipitation and temperature are two  
53 major components of a changing climate that have been analyzed extensively over the  
54 past two decades (Trenberth and Shea 2005; Li et al., 2009; Kharin et al., 2013).  
55 According to the United Nations Office for Disaster Risk Reduction UNISDR (2015),  
56 India is the third most influenced nation by weather related by disasters, which can  
57 largely be attributed to both higher occurrences of extreme temperatures and precipitation.  
58 Recently, Trenberth (2005) showed that climate change due to increased greenhouse gas  
59 emissions leads to changes in extreme event behavior in terms of precipitation and  
60 temperature all over the world. Generalized Extreme Value (GEV) statistical distribution  
61 has long been used to examine time-series of climate extremes with different return levels  
62 using three extreme value distributions that were proposed by Fisher and Tippet (1928).  
63 The three distributions are referred to as Gumbel, Frechet, and negative Weibull, which  
64 are discussed in Section 2. Jaruskova and Rencova (2008) studied the extreme changes in  
65 annual maxima and minima temperature series using five meteorological sites,  
66 implementing extreme value theory and hypothesis testing within the framework of the  
67 GEV-based method.

68 Jenkinson (1955) used GEV distribution for extreme precipitation events, which  
69 offered extensive adaptability of the three extreme value distributions. Later, several  
70 researchers used GEV statistical distribution to study extreme precipitation for many  
71 regions and different countries around the world (Fowler and Kilsby 2003; Nadarajah  
72 2005; and Gilleland and Katz 2006). In China, a warming trend has been confirmed in



73 both annual minimum and maximum temperature in the twentieth century (Choi et al.  
74 2009; You et al. 2011). Later studies also showed notable extreme temperature increases  
75 in northeastern China, and the smallest increase in the southern region (Liu et al. 2004).  
76 The frequency of extreme temperature events in China is expected to increase at an  
77 accelerating rate based on Coupled Model Inter-comparison Project (CMIP) historical  
78 projections (Wang and Chen 2014; Yang et al. 2014). Utilization of GEV distribution on  
79 temperature and precipitation over China has been extensively studied in several  
80 investigations (Wang and Zhou 2005; Zhang et al. 2011; Yang et al. 2014). As for India,  
81 Shashikanth et al. (2017) applied a GEV distribution to GCM summer monsoon  
82 precipitation in India during 1961-1990 and 2081-2100. They found a slight increase in  
83 the future extreme spatial mean in the later period. However, the statistical GEV  
84 distributions of extreme minimum and maximum temperatures in India have not been  
85 examined in any previous studies. We utilize this method over India to address this issue.  
86 CMIP models and observations are discussed in Section 2. The GEV statistical  
87 distribution methodology is described in Section 3. Section 4 presents the results of the  
88 GEV distribution in three different periods and occurrences over India, and finally the  
89 conclusions are discussed in Section 5.

## 90 **2. Data and Method**

91 The observational dataset of gridded monthly precipitation (P), minimum and  
92 maximum surface temperatures ( $T_{\min}$  and  $T_{\max}$ ) are taken from the study of the Climate  
93 Research Unit (CRU TS3.1) described by Harris et al. (2014). The datasets are collected  
94 from 1901 to 2005 over land areas, based on daily values from rain gauge measurements  
95 provided by more than 4,000 weather stations distributed around the world (New et al.,



1999, 2000). The precipitation and surface temperatures are collected from different sources, with rigorous quality checking procedures before gridding (Mitchell and Jones, 2005; Harish et al., 2014). Figure 1 shows the Indian map with seven regions.

The monthly precipitation, and the minimum and maximum surface temperatures ( $T_{\min}$  and  $T_{\max}$ ) are simulated by CMIP5 (Coupled Intercomparison Project Phase 5) models for a historical (hereafter referred to as "Historical") period from 1850 to 2005 (Smith et al., 2013; Lamarque et al., 2010) as well as the 21st century (years 2006-2100) employing four different representative concentration pathways (RCPs) (Moss et al., 2010, Taylor et al., 2012). The Historical and different scenarios of CMIP5 models are listed in Table 1. Further details on the models and their configuration are described in the references, online at <http://www-pcmdi.llnl.gov/>. We have considered only models for which the same ensemble member i.e. 'r1i1p1' is available both in the historical and four (RCP2.6, RCP4.5, RCP6.0, and RCP8.5) scenarios considered here. According to the IPCC Fifth Assessment Report, the CMIP5 models exhibit improvements in the simulations especially surface temperature and precipitation compared to the previous climate models (Flato et al. 2013). The outputs for both historic and different RCPs outputs are available on different spatial scales, which are consequently regridded to a common spatial scale of  $1^\circ$  in latitude and  $1^\circ$  in longitude resolution.

Out of the monthly CMIP5 model outputs (listed in Table 1), Historical experiments, RCP (2.6, 4.5, 6.0, and 8.5) experiments of  $T_{\min}$ ,  $T_{\max}$ , and Precipitation (P) are utilized for our analysis.



Three types of extreme distributions compose a GEV distribution: Gumbel, Frèchet, and Weibull, also known as type I, II, and III respectively (Martins and Stedinger 2000; Feng et al., 2007). These can generally be described by

$$G(z; \mu, \sigma, \xi) = \begin{cases} \exp\left\{-\exp\left[-\left(\frac{z-\mu}{\sigma}\right)\right]\right\}, & \xi = 0 \\ \exp\left\{-\left[1 + \xi \frac{z-\mu}{\sigma}\right]^{-\xi^{-1}}\right\}, & \xi \neq 0, 1 + \xi \frac{z-\mu}{\sigma} > 0 \end{cases} \quad (1)$$

where  $\mu$ ,  $\sigma$  and  $\xi$  are the location, scale, and shape parameters, respectively. Particular cases of Eq. (1) with  $\xi \rightarrow 0$ ,  $\xi > 0$ , and  $\xi < 0$  correspond to the Gumbel, Frèchet, and the negative Weibull distributions, respectively. Generally, the value of  $\xi$  is greater than zero for precipitation data, although the distribution of Gumbel is sometimes adequate.

Several methods have been developed for the estimation of the parameters of GEV distributions. These include the method of moments by Christopheit (1994), the less influenced method of L-moments (Hosking, 1990; Hosking and Wallis, 1997); the Bayesian method by Smith and Naylor (1987), Coles and Tawn (2005). The most popular method is the maximum likelihood method (Smith and Naylor, 1987; Unkašerić and Tošić, 2009), which has the advantage of allowing the addition of fitting co-variables (such as trends, cycles or physical variables) (Katz et al., 2002). The detailed procedure of these methods summarized by the El Adlouni et al. (2007), Kioutsioukis et al. (2010), and Kharin et al. (2013). In this study, the maximum likelihood method is used to estimate the parameters of the GEV distribution. The regression parameters of  $\mu(t)$ ,  $\sigma(t)$ , and  $\xi(t)$  are the location, scale, and shape respectively. The parameters of the likelihood function, given  $n$  observations  $\{(t_1, z_1), (t_2, z_2), \dots, (t_n, z_n)\}$  at period  $t_i$  at which the greatest  $z_i$  is acquired, is provided by



$$L(\theta|t_t, z_t) = \prod_{i=1}^m g[z_i; \mu(t_i), \sigma(t_i), \xi(t_i)] \quad (2)$$

where

$$g(z; \mu, \sigma, \xi) = \frac{1}{\sigma} \left\{ \left[ 1 + \xi \left( \frac{z - \mu}{\sigma} \right) \right]^{-(1+1/\xi)} \right\} \exp \left\{ - \left[ 1 + \xi \left( \frac{z - \mu}{\sigma} \right) \right]^{-1/\xi} \right\} \quad (3)$$

The log-likelihood function is

$$l(\theta|t_t, z_t) = -\sum_{i=1}^m \left\{ \log \sigma(t_i) + \left( 1 + \frac{1}{\xi(t_i)} \right) \log \left[ 1 + \xi(t_i) \left( \frac{z_i - \mu(t_i)}{\sigma(t_i)} \right) \right] + \left[ 1 + \xi(t_i) \left( \frac{z_i - \mu(t_i)}{\sigma(t_i)} \right) \right]^{-1/\xi(t_i)} \right\} \quad (4)$$

$\sigma(t_i) > 0$  and  $\{1 + \xi(t_i)(z_i - \mu(t_i))/\sigma(t_i) > 0\}$  for  $i=1, \dots, n$ . For every value of  $\xi(t_i)$

that equals to zero, it is important to utilize the suitable limiting form, replacing the GEV

by the Gumbel (Eq. (1) for  $\xi = 0$ ) log-likelihood function,

$$l(\theta|t_j, z_j) = -\log \sigma(t_j) - \frac{z_j - \mu(t_j)}{\sigma(t_j)} - \exp \left[ -\frac{z_j - \mu(t_j)}{\sigma(t_j)} \right] \quad (5)$$

The maximum likelihood estimate of  $\theta$  yields the maximization of Eq. (4) and/or Eq. (5).

Rao (1973) estimated the confidence intervals for the selected return periods using the

delta method. Figure 1 shows the regression, model fits and estimated the return values of

monthly maximum temperatures.

We implement this GEV analysis to study the minimum and maximum surface

temperatures and precipitation as simulated by CMIP5 models in the historical

experiments (years 1901-2005), CRU observations, and experiments for the 21st century

(years 2006-2100) with four different radiative forcing scenarios.

### 3. Results

#### 3.1 CMIP Historical and CRU temperature extremes



159           The spatial distribution of extremes for the Historical runs in India during 1901-  
160   2005 is presented by showing maximum and minimum temperature extremes with  
161   different return time periods are shown in Figure 2. The top and bottom panels show  
162   maximum and minimum extremes respectively with return periods of 10, 20 and 50 years,  
163   denoted as  $T_{(\max,10)}$ ,  $T_{(\max,20)}$ , and  $T_{(\max,50)}$  for maximum temperatures and  $T_{(\min,10)}$ ,  $T_{(\min,20)}$ ,  
164    $T_{(\min,50)}$ , for minimum temperatures respectively. The regional mean value for each return  
165   time period is mentioned at the top of each plot. The mean values indicate high warm  
166   extreme temperature conditions in India with average values of 34.89, 36.42, and 38.14°C  
167   for  $T_{(\max,10)}$ ,  $T_{(\max,20)}$ , and  $T_{(\max,50)}$  respectively. The mean CRU extreme regional values  
168   are 34.80, 36.46, and 38.42°C for the 10, 20, and 50 year periods (Figure not shown).  
169    $T_{(\max,10)}$  and  $T_{(\max,20)}$  show the most evident warm extremes over Northwest and North-  
170   central regions. These extreme regions extend to the Interior peninsula at  $T_{(\max,50)}$ . Similar  
171   extreme warm surface temperatures are observed over the northwestern part of India  
172   (Gadgil, 2018). These three regions show maximum extremes with return values all  
173   above 40°C, while the Western Himalaya region exhibits the lowest maximum  
174   temperature extremes at about 10°C. At  $T_{(\max,10)}$  large cold extremes cover most parts of  
175   the Western Himalaya region and slowly turn to warming extremes at  $T_{(\max,50)}$ . The  
176   minimum temperature extremes show large variations over India except for the Western  
177   Himalaya region. The mean value of minimum temperature extreme over the entire  
178   region in India is 7.75, 4.19, and -1.57°C for three (10, 20 and 50-year) return periods,  
179   respectively. More extreme cold changes are observed in Figure 2 over the northeastern  
180   and western regions of India, and cold temperature extremes drop from 7°C to -20°C for





181 10 and 50 years period. The warmer and colder extremes of the minimum temperature are  
182 observed over southern and northern parts of India respectively.

### 183 **3.2 CMIP Historical and CRU changes in temperature extremes**

184 The spatial differences between CMIP and CRU warm and cold temperature  
185 extremes for the three return estimates of 10, 20, and 50 year periods are shown in Figure  
186 3. The upper and lower panels display the changes in warm and cold temperature  
187 extremes for three time periods respectively. The positive (red color) and negative (blue  
188 color) values in these diagrams indicate the warmest and coldest Historical extremes for  
189 the three different periods.

190 The difference between the warm extremes decreases slightly from the 10 to 50-  
191 year period over central and northern parts of India. Warm and cold bands are clearly  
192 observed over the southern regions of the warm extreme difference map. Looking at the  
193 cold extreme differences, a cold band (with a magnitude of  $\sim 4.5^{\circ}\text{C}$ ) is observed in the  
194 northwest region of India for the 50-year period, indicating that the CRU cold extremes  
195 are warmer than those of CMIP5 historical runs. The regional mean value decreases from  
196  $0.14$  to  $-0.20^{\circ}\text{C}$  for warm extremes and decreases from  $-0.55$  to  $-0.95^{\circ}\text{C}$  for cold extremes  
197 from 10 to 50 year periods. From Figure 3, the magnitude of the difference of cold  
198 extremes is little larger than those of the warm extremes for all three return periods over  
199 India. The mean value of warm and cold extreme differences are less than a degree  
200 indicating a fairly good agreement between the Historical and CRU temperatures for the  
201 three different return periods. Kharin et al. (2005, 2007) observed that the temperature  
202 differences between CMIP5 multi-model and ERA-Interim are generally larger for cold  
203 extremes than for warm extremes during the period from 1986 to 2005. Table 2



204 summarizes the warm and cold extreme temperature mean values for the 10, 20, and 50-  
205 year periods of each region for the CRU, Historical, as well as the differences between  
206 the two. It is evident from the table that the maximum warm extreme mean temperature is  
207 observed in the Interior Peninsula over the Historical ensemble and CRU temperatures  
208 for the 20- and 50-year return periods.

### 209 **3.4 Future climate extreme changes in CMIP5 projections**

210 The spatial GEV distribution for three different return values of 10, 20, and 50  
211 years estimated from CMIP5 maximum temperatures of different RCP scenarios (RCP  
212 2.6, 4.5, 6.0, and 8.5) for the period 2006-2099 are shown in Figure 4. All RCPs suggests  
213 comparable spatial distributions of maximum temperatures over the three different  
214 periods. The spatial distributions of warm extremes for all RCPs look similar in the 50-  
215 year period. Moderately warm regional mean temperature changes are observed in  
216 RCP2.6 and RCP8.5 scenarios at about 1.15, 1.28, and 1.28°C for the three (10, 20 and 50  
217 year) periods, respectively. In RCP2.6, the warm temperature extremes are observed in  
218 northwest (NW) and north central (NC) regions in the 10-year period, while warm  
219 extremes cover three regions (NW, NC, and IP) in the 20-year period, and most of the  
220 regions in India in the 50 year period. In RCP8.5 the maximum temperatures are  
221 observed in most of the Indian regions with regional means of 39.96, 39.99, and 41.18°C  
222 for the three (10, 20, and 50-year) return periods, respectively. Maximum extreme  
223 temperatures of about ~44°C are observed in several grids throughout India under (RCP  
224 2.6 and 8.5) CMIP5 experiments in the 20 and 50 year return periods. Similar extreme  
225 temperatures reach values of around 46°C in large areas of northwest and Interior  
226 peninsula regions over equatorward of 25°. All simulations demonstrate an ascent of



227 more than  $\sim 3.5^{\circ}\text{C}$  over three regions (NW, NC, and IP), and a warming of more than  $2^{\circ}\text{C}$   
 228 over the western Himalayan region in the 50 year period.

229 The spatial distribution of cold temperature extremes during the 21<sup>st</sup> century  
 230 under the RCP scenarios (RCP 2.6, 4.5, 6.0, and 8.5) for the three different time periods  
 231 over India are shown in Figure 5. The regional mean values of cold extremes have  
 232 consistently decreasing trends in all RCP scenarios. The northwest, western Himalayas,  
 233 and northeast are the main regions exhibiting diminishing trends in all three return  
 234 periods. The mean value of cold extremes for the 50-year period is  $\sim 7^{\circ}\text{C}$  higher than the  
 235 20-year period for RCP2.6. For the other concentration pathways (RCP 4.5, 6.0 and 8.5),  
 236 the projected increase in cold temperature extremes ranges from  $2.5^{\circ}\text{C}$  to  $2.8^{\circ}\text{C}$ , and  $3.3^{\circ}\text{C}$   
 237 to  $3.9^{\circ}\text{C}$  over the period 10 to 20 and 20 to 50-year return periods, respectively. Note  
 238 that the positive changes of about  $\sim 5^{\circ}\text{C}$  in temperature are observed in the RCP8.5  
 239 experiment in 21st century relative to the 1901-1960 historic period (Basha et al., 2017).  
 240 The cold temperature extreme slowly decreases with latitude from south to north of India  
 241 in all RCP scenarios. The magnitude at the southern tip of India is about  $20^{\circ}\text{C}$ , which  
 242 decreases to  $-23^{\circ}\text{C}$  over the northern tip. The maximum regional cold extreme value at  
 243 about  $12.73^{\circ}\text{C}$  is observed in RCP8.5 for a 10-year period, while the minimum at about -  
 244  $0.99^{\circ}\text{C}$  is observed in RCP2.6 for 50-year return period.

### 245 **3.5 Temperature extremes inter-model uncertainty in CMIP5 projections:**

246 The variability of the warm and cold temperature extremes over India can be  
 247 shown by standard deviations as shown in Figures 6 and 7, which depict the spatial  
 248 distributions of standard deviations for three different time periods (10, 20, and 50-year)  
 249 of warm ( $T_{\max}$ ) and cold ( $T_{\min}$ ) extremes projected in the four different scenarios (RCP2.6,



250 4.5, 6.0, and 8.5), respectively. The spatial map in Figure 6 indicates the maximum to be  
251 in the southern part of Interior Peninsula (IP), while the second maximum (relatively  
252 weak) is at the Western Himalaya (WH) region in RCP2.6 at the 50-year period. The  
253 standard deviation of warm extremes is larger in the 50-year period compared to the 10-  
254 and 20-year periods especially in the southern part of India in all RCP scenarios. The  
255 maximum mean value is about  $0.75^{\circ}\text{C}$  in RCP8.5 (10-year period), whereas the minimum  
256 value is observed in RCP2.6 (50-year return value) at about  $0.33^{\circ}\text{C}$ . The standard  
257 deviations change in small increments across different scenarios for all return periods.  
258 For example, the standard deviation changes in 20-year return values are 0.47, 0.45, 0.41,  
259  $0.49^{\circ}\text{C}$  under RCP2.6, 4.5, 6.0, and 8.5 scenarios, respectively.

260 The spatial distribution of different CMIP5 experiments for three different time  
261 periods (10, 20, and 50-year) return values of cold extreme ( $T_{\min}$ ) standard deviations are  
262 shown in Figure 7. A distinct feature of warm bias (up to  $3.5^{\circ}\text{C}$ ) in eastern and western  
263 regions of India is observed in all scenarios at 20- and 50-year periods. In cold extremes,  
264 the 50-year return period standard deviation is higher compared to other return values  
265 under RCP2.6. The maximum mean value of  $T_{\min,50}$  is about  $2.29^{\circ}\text{C}$  in RCP2.6, while the  
266 minimum value ( $T_{\min,10}$ ) is observed in RCP8.5. The cold extremes have a larger  
267 variability comparing to warm temperature extremes. The mean maximum value of warm  
268 temperatures ( $T_{\max,50}$ ) is almost three times as large as the  $T_{\min,50}$  in RCP2.6. The  
269 variability of warm extremes (given by the standard deviation) are spatially fairly  
270 uniform in all the return periods, which is not the case for cold extremes under CMIP5  
271 scenarios. Recent observational (Lee et al., 2014) and modeling (Kharin et al., 2007,  
272 2013) studies have reported larger variability of warming in cold extremes compared to



273 warm extremes across different return periods. This indicates that variability in cold  
274 temperature extremes is larger than those of warm temperature extremes over India.

## 275 **4. Precipitation extremes**

### 276 **4.1 Historical and CRU precipitation extremes and differences**

277 The spatial variations of Historical (top panel), CRU (middle panel), and the  
278 differences between the two (bottom panel) of extreme precipitation for three different  
279 return periods (10, 20, and 50-year) are shown in Figure 8. The three (10, 20, and 50-  
280 year) periods of precipitation extremes are computed from the GEV procedure by using  
281 monthly precipitation grids. From Figure 8, precipitation extremes increase significantly  
282 from the 10 to the 50-year period in both Historical and CRU observations. In  
283 CMIP5\_historical runs the extreme precipitation appears to have a positive trend in the  
284 Interior Peninsula, which extends slightly into North Central (NC) part of India. The  
285 maximum trends, however is concentrated in the IP region. In the case of CRU, the  
286 increasing trend is observed over the IP and NC regions for the 20-year period, which  
287 also extends to most parts of India except for the southern tip and the Western Himalayan  
288 regions for the 50-year period. A widespread increase in extreme precipitation is  
289 observed in CRU for the 50-year period over the IP, NC, WC and EC regions. The  
290 differences between Historical and CRU extreme precipitations indicate that the CRU  
291 extreme values are slightly higher over the IP and NC, while Historical is slightly higher  
292 in the northern and southern parts of India for the 10- and 20-year periods. In the 50-year  
293 period, precipitation is higher in the Historical runs compared to CRU over the Interior  
294 Peninsula, Western Himalayan regions. However, extreme precipitation is lower in the  
295 Historical runs, in the northwest and extending to northwest and extending to north-



central regions of India. The regional mean differences are -11.89%, -11.33% and 4.69% for all three (10, 20, and 50-year) periods, respectively.

The multi-model extreme precipitation differences for the 10-, 20-, and 50-year return periods during the period 2006-2100 for each CMIP5 scenarios (RCP2.6, 4.5, 6.0, and 8.5) relative to the 1901-2005 historical periods are shown in Figure 9. The northwestern region has the greatest decrease in all CMIP5 scenarios for all three return periods, which implies that the warmest region has the greatest decrease in extreme precipitation in future projections. The maximum mean difference is about ~23% in RCP8.5 for the 50-year return period. In comparison, future projections of extreme precipitation are slightly higher than Historical ones in the northern and some regions within Interior Peninsula. However, the Historical precipitation extremes are dominant in the 50-year period, and to a smaller extent in the 10-year period. The regional mean changes of extreme precipitation for the 50-year period are -10.4%, -12.9%, -4.3%, and -22.9% under the RCP2.6, 4.5, 6.0, and 8.5 scenarios, respectively. From Figure 9, the regional mean changes of future precipitation extremes are 1.9% and 5.9% in RCP2.6 (20-year period) and RCP6.0 (20-year period), respectively. Shashikanth et al. 2017 also found that significant changes in monsoon precipitation extremes during a 30-year period (2081-2100) compared to the historic period.

## 5. Conclusions

We have assessed the Historical and CRU precipitation and temperature extremes and likely future changes within them throughout India. We quantified the warm and cold temperatures as well as precipitation extremes of CMIP5 for all Representative Concentration Pathway scenarios (RCP2.6, 4.5, 6.0, and 8.5) for the future using a



319 statistical model of climate extremes based on GEV distributions for the three return  
320 periods (10, 20, and 50-year). The most important findings of our analysis are  
321 summarized as follows:

322 Extreme warm values in Historical  $T_{\max}$  in India appear to be rather moderate.  
323 The regional means of extreme maximum temperatures are 34.89, 36.42, and 38.14 °C for  
324 all three (10, 20, and 50-year) return periods, respectively, while the minimum extreme  
325 temperatures are 7.75, 4.19, -1.47 °C for those same return periods. Comparing the 10- to  
326 50-year return periods, the warm extremes increase at about ~3 °C over northwestern,  
327 north central, and Interior peninsula regions. Cold extremes are decreased ~5 °C  
328 especially over the eastern and western regions of India.

329 The regional relative mean differences of Historical and CRU  $T_{\max}$  extremes are  
330 0.14, 0.01 and -0.20 °C for the three (10, 20, and 50-year) periods, respectively.  
331 Comparing the 10- and 50-year return periods shown that the relative changes of extreme  
332 temperatures decrease in Northwest, North central, and northern part of Interior peninsula,  
333 and increase over lower part of the west coast. The relative mean differences of CRU  
334 cold extremes are slightly higher than those of the Historical runs. The relative mean  
335 differences of cold extremes are -0.55, -0.64, and 0.28 °C for the three (10, 20, and 50-  
336 year) periods, respectively. CRU shows more changes in the cold extremes as opposed to  
337 warm extremes compared to the Historical extremes. Regionally, northwestern and  
338 northeastern regions of India show the highest changes.

339 Future  $T_{\max}$  extreme temperatures increase in all RCP scenarios compared to  
340 historical temperatures, especially for the 20 and 50 year periods. The regional extreme  
341 mean values increase moderately compared to the historical values at about 1.85 and 2.92



342 °C in the 50-year period under RCP6.0 and 8.5 scenarios. In the case of  $T_{\min}$  extreme  
343 mean temperatures of RCP2.6 decrease by nearly 5 °C compared to the historical values,  
344 while the minimum extreme temperature mean in RCP8.5 increase by nearly 4 °C  
345 compared to historical temperatures in 50-year return period. It must be noted that the  
346 effect of increasing radiative forcing under higher concentration pathways is larger on  
347 cold temperatures compared to warm temperatures.

348         The spatial variability of CRU extreme precipitation rates is substantially larger  
349 compared to Historical extremes in all three return periods. Upon comparing 10-, and 50-  
350 year periods, changes in precipitation extremes are observed in both the location and  
351 scale of the distribution, especially over North Central and Interior Peninsula regions of  
352 India. In the other regions, CRU precipitation extreme changes increase slightly in the  
353 50-year period. The regional mean relative difference of Historical and CRU precipitation  
354 extremes is observed the 50-year period at about -14.6%. It indicates that Historical  
355 precipitation extremes show smaller values compared to CRU in several regions in India.  
356 The past and future differences of extreme precipitation are significantly larger when  
357 comparing to Historical to RCP8.5, implying that increasing radiative forcing under  
358 higher greenhouse gas concentrations may lead to larger changes in precipitation  
359 extremes.

### 360 **Acknowledgements**

361         We acknowledge the GCM modeling groups, the Program for Climate Model  
362 Diagnosis and Inter-comparison (PCMDI), and the WCRP's Working Group on Coupled  
363 Modeling for their roles in making available WCRP CMIP5 multi-model datasets. The





364 authors would like to thank the National Center for Atmospheric Research (NCAR) for  
365 providing the CRU data.

### 366 **Figure captions**

367 Figure 1. Sample plot of Generalized Extreme Value (GEV) distribution return values,  
368 empirical and modeled fits with 95% confidence level, together with the map of  
369 India divided in the seven regions used in this study.

370 Figure 2. The historical maximum temperature ( $T_{\max}$ ; top panel), and minimum  
371 temperature ( $T_{\min}$ ; bottom panel) extremes for 10-year (left), 20-year (middle),  
372 and 50-year (right) periods during 1901-2005.

373 Figure 3. The difference between CMIP5\_historical and CRU maximum temperature  
374 ( $T_{\max}$ ; top panel), and minimum temperature ( $T_{\min}$ ; bottom panel) extremes for  
375 (left) 10-year, (right), 20-year, and (right) 50-year periods during 1901-2005.

376 Figure 4. The (left) 10-year, (middle) 20-year, and (right) 50-year return values of CMIP5  
377 multi-model mean of warm temperature extremes for the period 2006-2100  
378 under RCP2.6 (1<sup>st</sup> row), RCP4.5 (2<sup>nd</sup> row), RCP6.0 (3<sup>rd</sup> row), and RCP8.5  
379 (bottom row) scenarios, together with the regional average stated on top of each  
380 panel.

381 Figure 5. The (left) 10-year, (right) 20-year, and (right) 50-year return values of CMIP5  
382 multi-model minimum temperature extremes projected in 2006-2100 under  
383 RCP2.6 (1<sup>st</sup> row), RCP4.5 (2<sup>nd</sup> row), RCP6.0 (3<sup>rd</sup> row), and RCP8.5 (bottom  
384 row) experiments, together with the regional means stated on top of each panel.

385 Figure 6. The CMIP5 inter-model standard deviations for the 10-year (left), 20-year  
386 (middle), and 50-year (right) return values of warm temperature extremes



387 simulated in the RCP2.6 (1<sup>st</sup> row), RCP4.5 (2<sup>nd</sup> row), RCP6.0 (3<sup>rd</sup> row), and  
 388 RCP8.5 (bottom row) experiments, respectively.

389 Figure 7. The CMIP5 inter-model standard deviations for the 10-year (left), 20-year  
 390 (middle), and 50-year (right) return values of cold temperature extremes  
 391 simulated in the RCP2.6 (1<sup>st</sup> row), RCP4.5 (2<sup>nd</sup> row), RCP6.0 (3<sup>rd</sup> row), and  
 392 RCP8.5 (bottom row) experiments, respectively.

393 Figure 8. The 10-year (left), 20-year (middle), and 50-year (right) return values of  
 394 Historical (1<sup>st</sup> row), CRU (2<sup>nd</sup> row), and the relative change between Historical  
 395 and CRU (% , bottom row) of precipitation extremes during 1901-2005.

396 Figure 9. The CMIP5 multi-model mean relative change (%) for the 10-year (left), 20-  
 397 year (middle), and 50-year (right) return values of precipitation extremes  
 398 between the historic values in 1901-2005 and the simulated values in 2006-2100  
 399 under RCP2.6 (1<sup>st</sup> row), RCP4.5 (2<sup>nd</sup> row), RCP6.0 (3<sup>rd</sup> row), and RCP8.5  
 400 (bottom row) scenarios, together with their regional means of relative changes  
 401 on top of each panel.

402  
 403  
 404  
 405  
 406  
 407  
 408  
 409



## 410 References:

- 411 Choi, G., Collins, D., Ren, G. Y. et al.: Changes in means and extreme events of  
412 temperature and precipitation in the Asia- Pacific network region, 1955-2007. Int.  
413 J. Climatol., 29, 1906-1925, 2009.
- 414 Fisher R. A., and Tippet, L. H. C.: Limiting forms of the frequency distribution of the of  
415 a sample, Proce. Cambridge Philos. Soc., 180-190,1928
- 416 Flato, G., Marotzke, J., Abiodun, B., Braconnot, P., Chou, S. C., Collins, W., Cox, P.,  
417 Driouech, F., Emori, S., Eyring, V., Forest, C., Gleckler, P., Guilyardi, E., Jakob,  
418 C., Kattsov, V., Reason, C., Rummukainen, M.: Evaluation of climate models. In:  
419 Stocker TF et al (eds) Climate Change 2013: the physical science basis,  
420 Cambridge University Press, Cambridge, 741-866, 2013.
- 421 Flower, H. J., and Kilsby, C. G.: A regional frequency analysis of United Kingdom  
422 extreme rainfall from 1961to 2000, International Journal of Climatology, 23(11),  
423 1313-1334. doi: 10.1002/(ISSN)1097-0088, 2003.
- 424 Gadgil, S.: The monsoon system: Land-sea breeze or the ITCZ?. J. Earth Syst. Sci., 5,  
425 127. doi:10.1007/s12040-017-0916-x, 2018.
- 426 Gilleland, E., Katz, R.: Analyzing seasonal to interannual extreme weather and climate  
427 variability with the extremes toolkit. In 18<sup>th</sup> Conference on Climate Variability  
428 and Change, 86<sup>th</sup> American Meteorological Society (AMS) Annual Meeting, 20  
429 January – 2 February, 2006, Atlanta, Georgia, 2006.
- 430 Harrish, I., Jones, P., Osborn, T., and Lister, D.: Updated high resolution grids of  
431 monthly climate observations-The CRU TS3.10 dataset, Int. J. Climatol., 34, 623-  
432 642. doi: 10.1002/joc.3711, 2014.
- 433 Jaruskova, D., and Rencova, M.: Analysis of annual maximum and minimal temperatures  
434 for some European cities by change point methods, Environmetrics, 19(3), 221-  
435 233. doi: /10.1002/env.865, 2008.
- 436 Jenkinson, A. F.: The frequency distribution of the annual maximum (or minimum)  
437 values of meteorological elements, Quart. J. Roy. Meteor. Soc., 81, 158-171, 1955.
- 438 Kharin, V. V., Zwiers, F. W., Zhang, X., and Hegerl, G. C.: Changes in temperature and  
439 precipitation extremes in the IPCC ensemble of global coupled model simulations,  
440 J. Climatol., 20, 1419-1444, 2007.



- 441 Kharin, V. V., and Zwiers, F. W.: Estimating extremes in transient climate change  
442 simulations, *J. Climatol.*, 18, 1156-1173, 2005.
- 443 Kharin, V. V., Zwiers, F. W., Zhang, X., and Wehner, M.: Changes in temperature and  
444 precipitation extremes in the CMIP5 ensemble, *Climate Change*, 119, 345-357,  
445 2013.
- 446 Lamarque, J. -F., Bond, T. C., Eyring, V., Granier, C., Heil, A., Klimont, Z., Lee, D.,  
447 Lioussé, C., Mievile, A., Owen, B., Schultz, M. G., Shindell, D., Smith, S. J.,  
448 Stehfest, E., Van Aardenne, J., Cooper, O. R., Kainuma, M., Mahowald, N.,  
449 McConnell, J. R., Naik, V., Riahi, K., and Van Vuuren, D. P.: Historical (1850-  
450 2000) gridded anthropogenic and biomass burning emissions of reactive gases and  
451 aerosols: Methodology and application, *Atmos. Chem. Phys.*, 10, 7017-7039.  
452 doi:10.5194/acp-10-7017-2010, 2010.
- 453 Li, L., Hong, Y., Wang, J. H., Adler, R. F., Policicelli, F. S., Habib, S., Irwn, D., Korme,  
454 T., Okello, L.: Evaluation of the real-time TRMM-based multi-satellite  
455 precipitation analysis for an operational flood prediction system in Nzoia basin,  
456 lake Victoria, Africa, *Natural Hazards*, 50, 109-123, 2009.
- 457 Liu, B. H., Xu, M., Henderson, M., et al.: Taking China's temperature: daily range,  
458 warming trends, and regional variations, *J. Climatol.*, 17, 4453-4462, 2004.
- 459 Mitchell, T. D., and Jones, P. D.: An improved method of constructing a database of  
460 monthly climate observations and associated high-resolution grids, *Int. J.*  
461 *Climatol.*, 25, 693-712, 2005.
- 462 Moss, R. H., Edmonds, J. A., Hibbard, K. A., Manning, M. R., Rose, S. K., Van Vuuren,  
463 D. P., Carter, T. R., Emori, S., Kainuma, M., Kram, T., Meehl, G. A., Mitchell, J.  
464 F. B., Nakicenovic, N., Riahi, K., Smith, S. J., Stouffer, R. J., Thomson, A. M.,  
465 Weyant, J. P., and Wilbanks, T. J.: The next generation of scenarios for climate  
466 change research and assessment, *Nature*, 463, 747-756. doi:10.1038/nature08823,  
467 2010.
- 468 Nadarajah, S.: Extremes of daily rainfall in west central Florida, *Climate Change*, 69,  
469 325-342, 2005.



- 470 New, M., Hulme, M., and Jones, P.: Representing twentieth century space-time climate  
471 variability. Part 1: development of a 1961-90 mean monthly terrestrial climatology,  
472 J. Climate, 12, 829-856, 1999.
- 473 New, M., Hulme, M., Jones, P. D.: Representing twentieth century space-time climate  
474 variability, II: development of 1901-1996 monthly grids of terrestrial surface  
475 climate, J. Climate, 13, 2217-2238, 2000.
- 476 Pickandas, J.: Statistical Inference Using Extreme Order Statistics, The Annals of  
477 Statistics, 3, 119-131, 1975.
- 478 Shashikanth, K., Ghosh, S., Vittal, H., and Karmakar, S.: Future projections of Indian  
479 summer monsoon rainfall extremes over India with statistical downscaling and its  
480 consistency with observed characteristics, Clim. Dyn., doi: 10.1007/s00382-017-  
481 3604-2, 2017.
- 482 Smith, T. M., Arkin, P. A., Sapiano, M. R. P.: Merged statistical analyses of historical  
483 monthly precipitation anomalies beginning 1990, J. Climatol., 23, 5755-5770,  
484 2010.
- 485 Taylor, K. E., Stouffer, R. J., and Meehl, G. A.: An overview of CMIP5 and the  
486 experiment design. Bull. Am. Meteorol. Soc., 93, 485-498. doi:10.1175/BAMS-  
487 D-11-00094.1, 2012.
- 488 Trenberth, K.E.: Uncertainty in hurricanes and global warming, Science, 308, 1753-1754,  
489 2005.
- 490 Trenberth, K.E., and Shea, D. J.: Relationships between Precipitation and Surface  
491 temperature, Geophys. Res. Lett., 32, L14703, doi: 10.1029/2005GL022760, 2005.
- 492 Wang, L., Chen, W.: A CMIP5 multi model projection of future temperature,  
493 precipitation, and climatological drought in China, Int. J. Climatol., 34, 2059-  
494 2078, 2014.
- 495 Wang, Y. Q., and Zhou, L.: Observed trends in extreme precipitation events in China  
496 during 1961-2001 and the associated changes in large-scale circulation. Geophys.  
497 Res. Lett., 32, 4, 2005.
- 498 Yang, S. L., Feng, J. M., Dong, W. J., and Chou, J.: Analysis of extreme climate events  
499 over China based on CMIP5 historical and future simulations, Adv. Atmos. Sci.,  
500 31, 1209-1220, 2014.



501 You, Q. L., Kang, S. C., Aguilar, E., et al.: Changes in daily climate extremes in China  
502 and their connection to the large scale atmospheric circulation during 1961-2003,  
503 Clim. Dyn., 36, 2399-2417, 2011.

504 Zhang, L., Dong, M., and Wu, T. W.: Changes in precipitation extremes over Eastern  
505 China simulated by the Beijing Climate Center Climate System Model  
506 (BCC\_CSM1.0), Clim. Res., 50, 227-245, 2011.

507  
508  
509  
510  
511  
512  
513  
514  
515  
516  
517  
518  
519  
520  
521  
522  
523  
524  
525  
526  
527  
528  
529  
530  
531  
532  
533  
534  
535  
536  
537  
538  
539  
540  
541  
542  
543



Table 1: Historical and CMIP5 different scenarios (RCP2.6, RCP4.5, RCP6.0, and RCP8.5) precipitation and maximum and minimum temperature

Model Name	Historical 1901-2005		CMIP5 2006-2099							
	Stem	Pr	Stem				Pr			
			RCP2.6	RCP4.5	RCP6.0	RCP8.5	RCP2.6	RCP4.5	RCP6.0	RCP8.5
CCSM4	Y	Y	Y	Y	Y	Y	Y	Y	Y	Y
CNRM-CM5	Y	Y	Y	Y	Y	Y	Y	Y	Y	Y
CSIRO-MK3	Y	Y	Y	Y	Y	Y	Y	Y	Y	Y
CanESM2	Y	Y	Y	Y	Y	Y	Y	Y	Y	Y
GFDL-CM3	Y	Y	Y	Y	Y	Y	Y	Y	Y	Y
GISS-E2-H	Y	Y	Y	Y	Y	Y	Y	Y	Y	Y
GISS-E2-R	Y	Y	Y	Y	Y	Y	Y	Y	Y	Y
HadGEM2-CC	Y	Y	Y	Y	Y	Y	Y	Y	Y	Y
HadGEM2-ES	Y	Y	Y	Y	Y	Y	Y	Y	Y	Y
IPSL-CM5A-LR	Y	Y	Y	Y	Y	Y	Y	Y	Y	Y
MIROC-ESM	Y	Y	Y	Y	Y	Y	Y	Y	Y	Y
MIROC5	Y	Y	Y	Y	Y	Y	Y	Y	Y	Y
MPI-ESM-LR	Y	Y	Y	Y	Y	Y	Y	Y	Y	Y
MRI-CGCM3	Y	Y	Y	Y	Y	Y	Y	Y	Y	Y
NorESM1-M	Y	Y	Y	Y	Y	Y	Y	Y	Y	Y
BCC-CSM1-1	Y	Y	Y	Y	Y	Y	Y	Y	Y	Y
INMCM4	Y	Y	Y	Y	Y	Y	Y	Y	Y	Y
GFDL-ESM2M	N	N	N	N	N	N	N	N	N	N
BNU-ESM	N	N	N	N	N	N	N	N	N	N
IPSL-CM5A-MR	N	N	N	N	N	N	N	N	N	N
CANESM2	Y	Y	Y	Y	Y	Y	Y	Y	Y	Y
FGOALS-g2	Y	Y	Y	Y	Y	Y	Y	Y	Y	Y
CESM1-CAM5	Y	Y	Y	Y	Y	Y	Y	Y	Y	Y

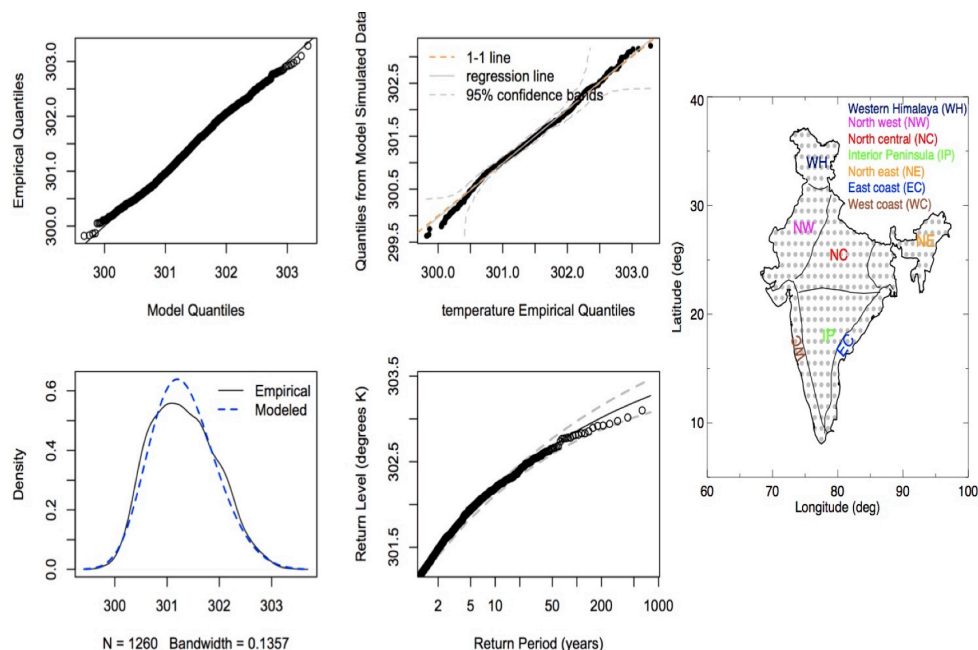


Table 2: CRU and differences between CRU and historical maximum and minimum temperature and standard deviation for seven homogeneous regions for 10-, 20-, and 50-year return periods.

Regions	CRU: $T_{max}$			CRU: $T_{min}$			CMIP - CRU: $T_{max}$			CMIP - CRU: $T_{min}$		
	Avg $\pm$ std			Avg $\pm$ std			Avg $\pm$ std			Avg $\pm$ std		
	10 year	20 year	30 year	10 year	20 year	30 year	10 year	20 year	30 year	10 year	20 year	30 year
India	34.80 $\pm$ 5.87	36.46 $\pm$ 6.15	38.42 $\pm$ 6.83	9.77 $\pm$ 8.07	6.51 $\pm$ 8.39	1.86 $\pm$ 10.04	0.14 $\pm$ 1.19	0.01 $\pm$ 1.05	-0.20 $\pm$ 1.46	-0.55 $\pm$ 0.82	-0.64 $\pm$ 0.31	-0.95 $\pm$ 2.12
IP	37.51 $\pm$ 1.59	40.12 $\pm$ 2.19	43.92 $\pm$ 3.33	15.55 $\pm$ 1.92	13.72 $\pm$ 2.53	11.51 $\pm$ 3.48	0.27 $\pm$ 1.06	0.09 $\pm$ 1.33	-0.30 $\pm$ 2.08	-0.35 $\pm$ 0.29	-0.75 $\pm$ 0.61	-1.52 $\pm$ 1.42
EC	35.62 $\pm$ 1.41	36.78 $\pm$ 1.63	38.08 $\pm$ 2.07	17.48 $\pm$ 2.90	15.17 $\pm$ 3.37	11.67 $\pm$ 6.42	-0.29 $\pm$ 2.03	-0.17 $\pm$ 1.96	0.01 $\pm$ 0.83	0.31 $\pm$ 0.49	0.31 $\pm$ 0.49	0.61 $\pm$ 0.95
NC	37.91 $\pm$ 2.82	39.81 $\pm$ 3.03	41.91 $\pm$ 3.44	9.76 $\pm$ 2.67	5.76 $\pm$ 3.42	0.19 $\pm$ 5.32	1.33 $\pm$ 1.51	0.77 $\pm$ 1.36	-0.13 $\pm$ 1.43	-0.28 $\pm$ 0.45	0.03 $\pm$ 1.03	0.57 $\pm$ 1.57
NW	38.13 $\pm$ 4.26	39.37 $\pm$ 4.33	40.47 $\pm$ 4.42	8.16 $\pm$ 3.06	3.98 $\pm$ 1.72	-1.54 $\pm$ 1.88	1.14 $\pm$ 0.56	0.85 $\pm$ 0.53	0.49 $\pm$ 0.51	-0.89 $\pm$ 0.69	-1.32 $\pm$ 0.76	-2.75 $\pm$ 3.86
WC	34.59 $\pm$ 2.27	35.83 $\pm$ 2.59	37.41 $\pm$ 3.18	16.44 $\pm$ 2.77	14.43 $\pm$ 3.03	11.63 $\pm$ 5.03	-0.33 $\pm$ 0.93	0.21 $\pm$ 1.22	1.37 $\pm$ 1.57	-0.01 $\pm$ 0.58	-0.64 $\pm$ 0.26	-2.28 $\pm$ 2.09
NE	30.46 $\pm$ 5.48	31.44 $\pm$ 5.65	32.31 $\pm$ 5.86	6.69 $\pm$ 5.78	1.10 $\pm$ 4.45	-8.99 $\pm$ 6.68	-1.33 $\pm$ 1.96	-1.42 $\pm$ 2.01	-1.54 $\pm$ 2.03	-0.93 $\pm$ 0.96	-0.69 $\pm$ 1.38	-0.11 $\pm$ 2.03
WH	18.14 $\pm$ 5.52	19.59 $\pm$ 5.36	20.74 $\pm$ 5.23	-13.75 $\pm$ 7.14	-15.71 $\pm$ 8.39	-17.53 $\pm$ 7.32	-2.28 $\pm$ 1.52	-1.63 $\pm$ 1.15	-0.89 $\pm$ 1.76	-2.02 $\pm$ 0.68	-1.87 $\pm$ 0.68	-1.67 $\pm$ 0.68

IP = Interior Peninsula; EC = East Coast; NC = North Central; NW = North West; WC = West Coast; NE = North East; WH = Western Himalayas.





**Figure 1**

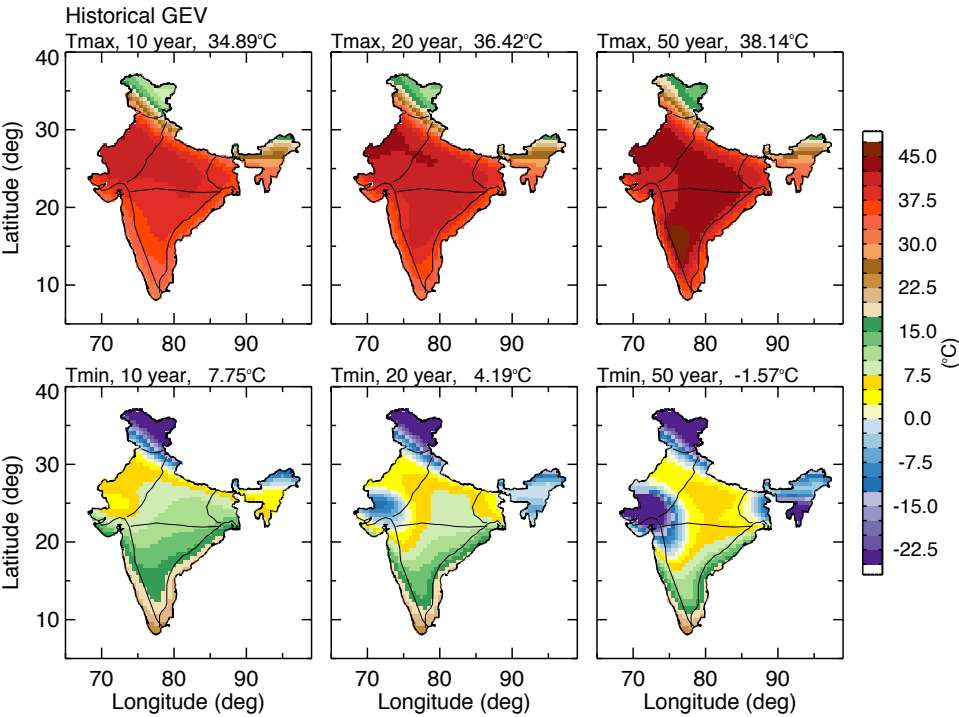
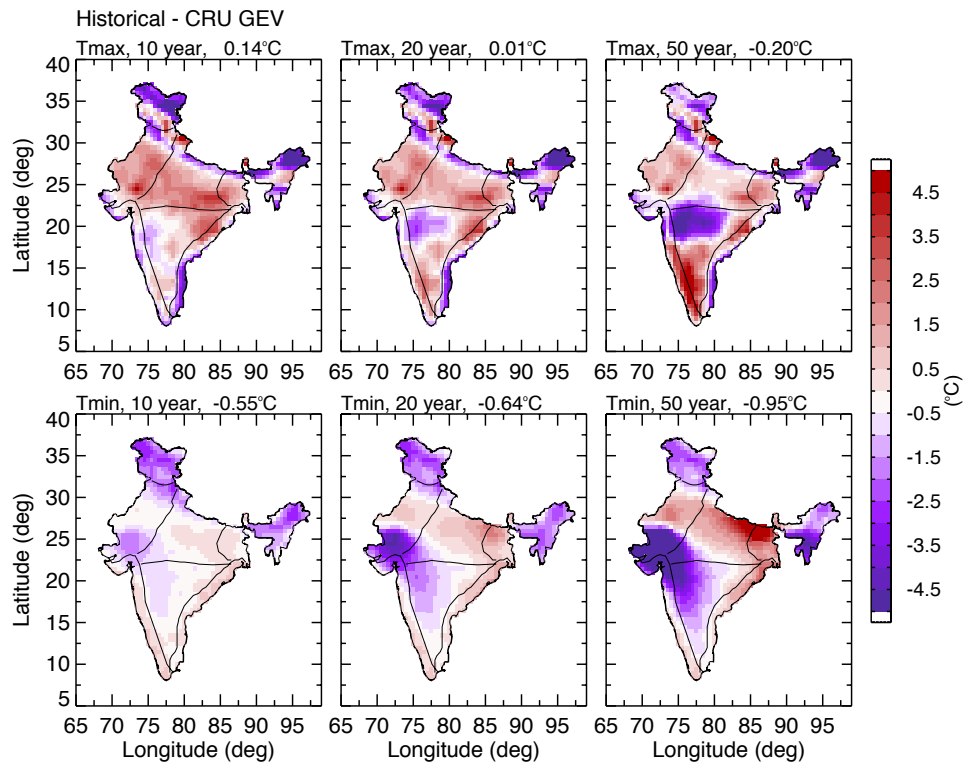


Figure 2



**Figure 3**

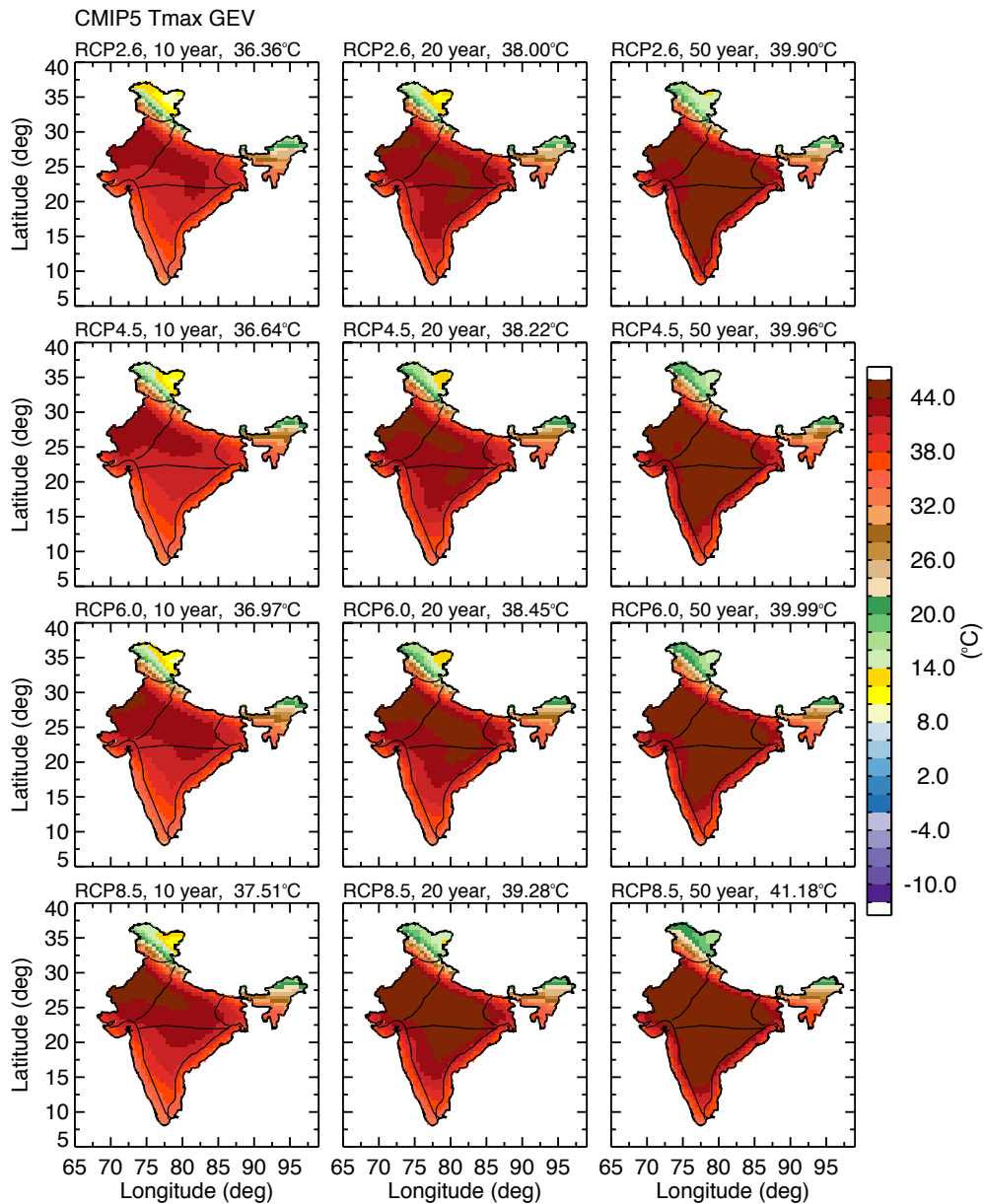


Figure 4

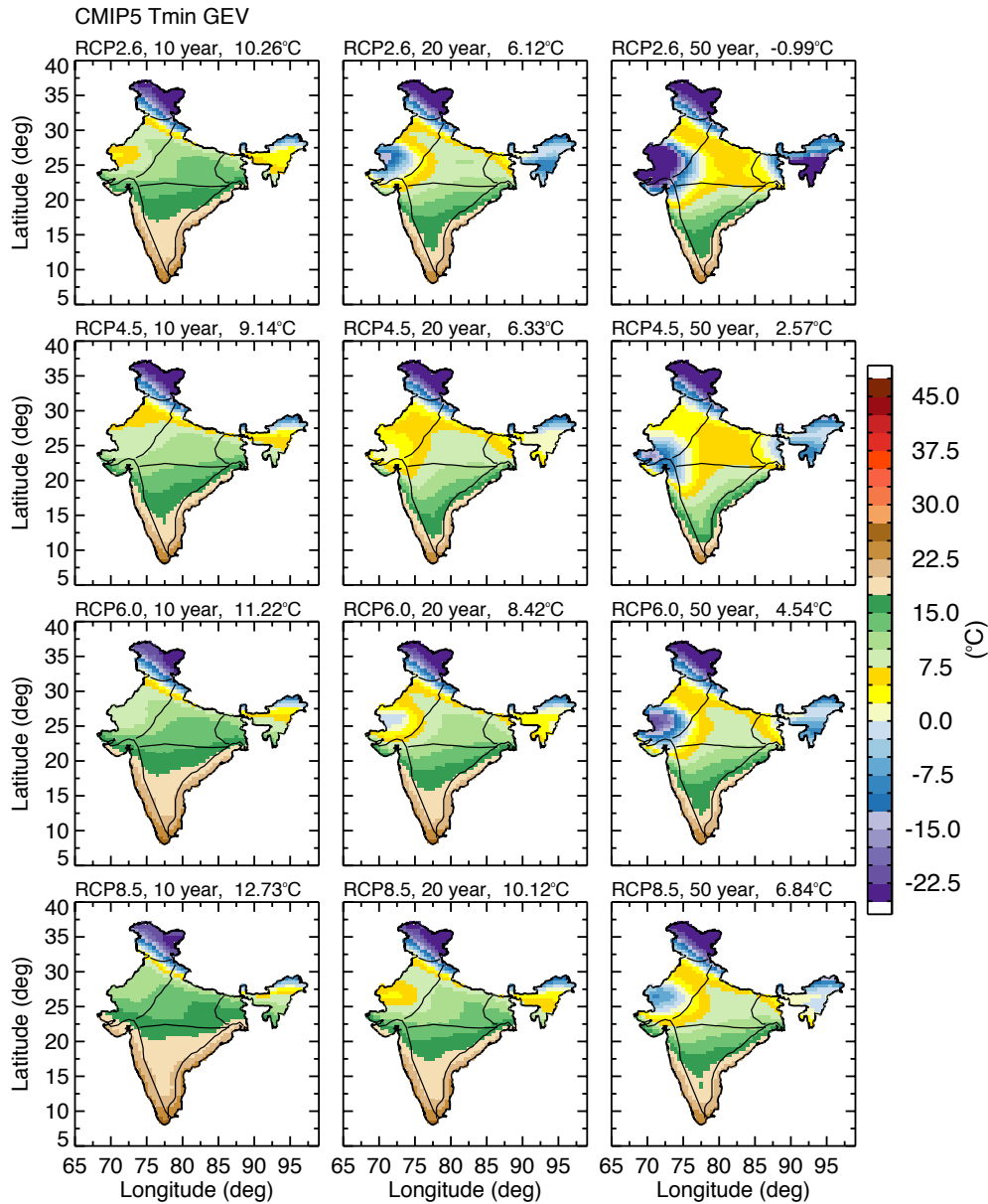


Figure 5

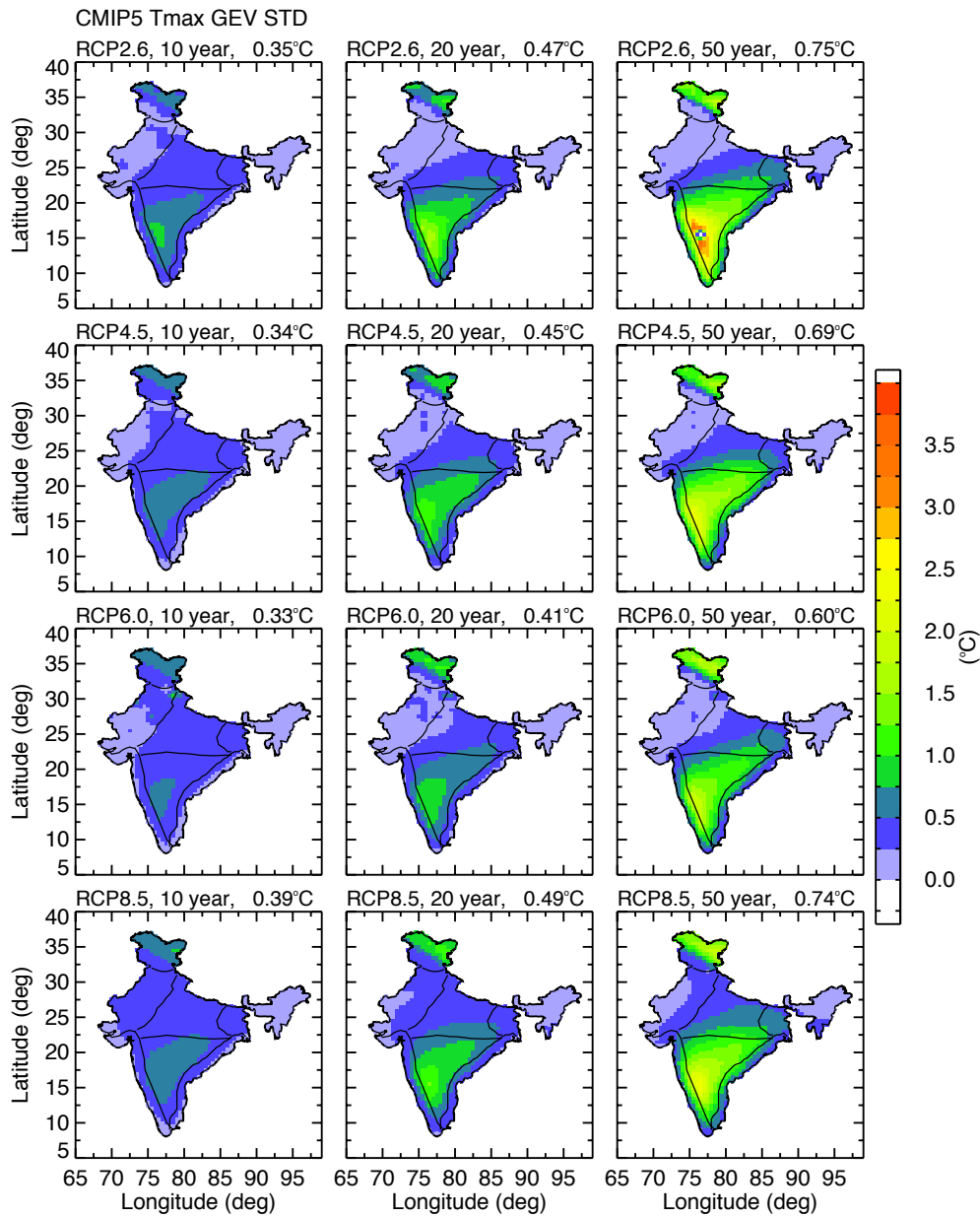


Figure 6

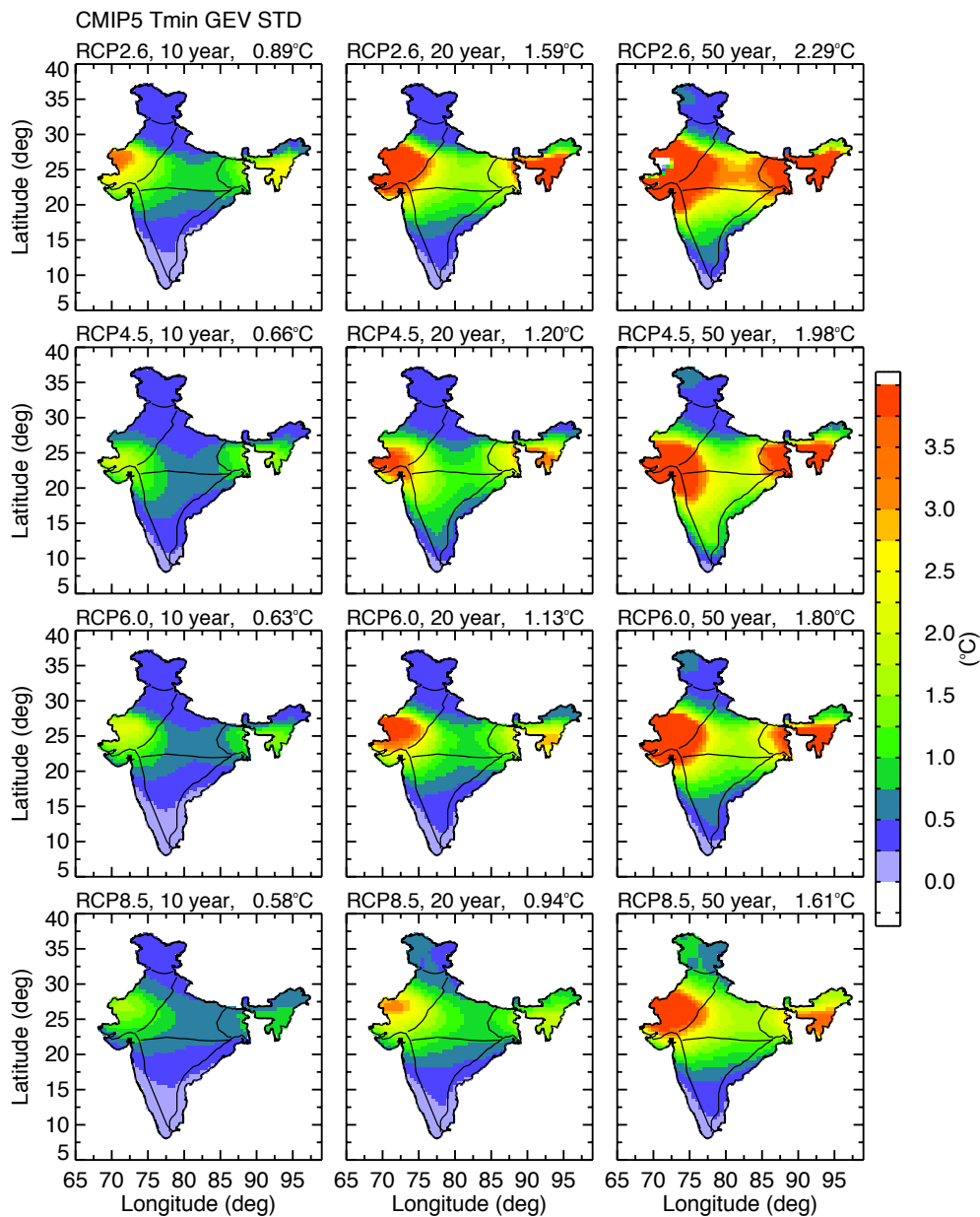


Figure 7

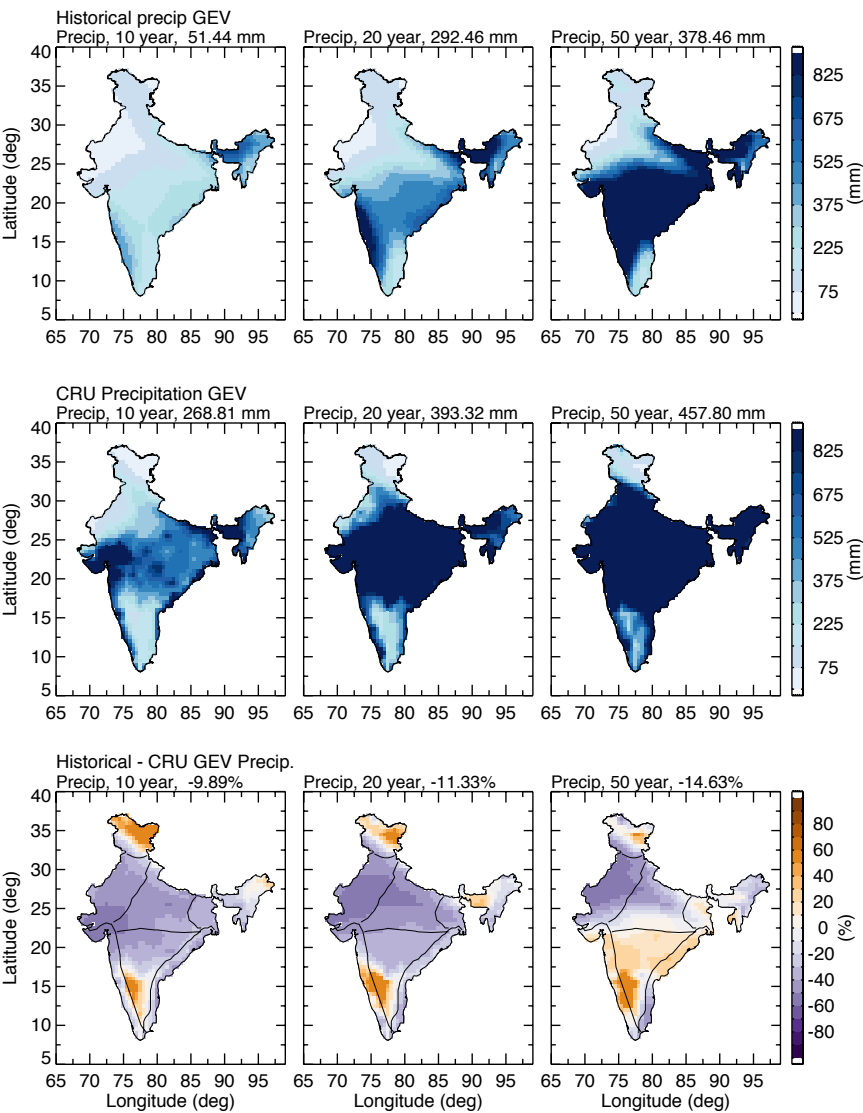
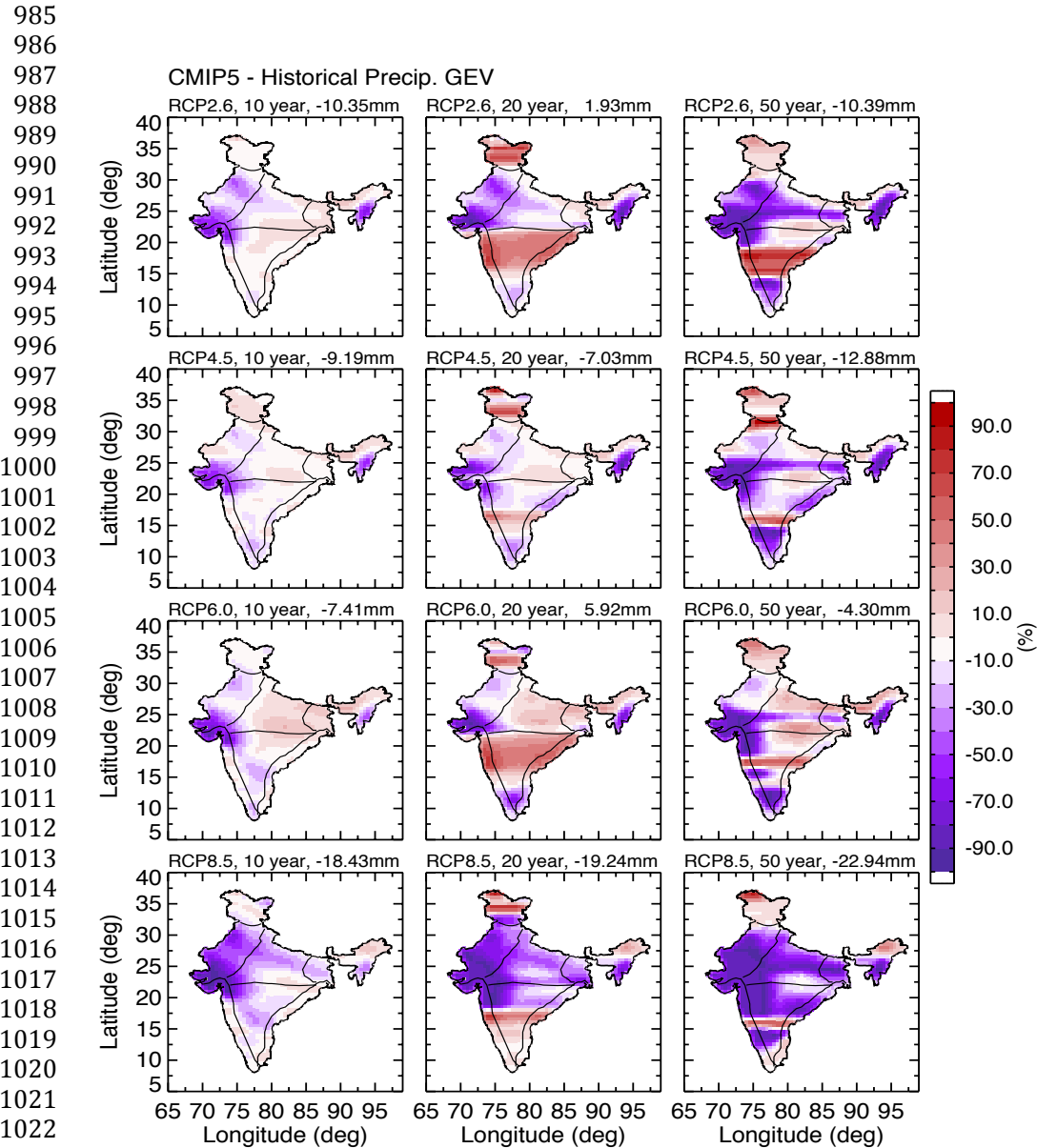


Figure 8





1024 **Figure 9**  
1025  
1026  
1027  
1028  
1029  
1030